Supplement of Biogeosciences, 21, 2691–2704, 2024
https://doi.org/10.5194/bg-21-2691-2024-supplement

Biogeosciences Open Access EGU

Supplement of

Molecular-level carbon traits of fine roots: unveiling adaptation and decomposition under flooded conditions

Mengke Wang et al.

Correspondence to: Sifang Kong (mengsiksf@163.com) and Junjian Wang (wangjj@sustech.edu.cn)

Text S1 Root sample collection

For soil-grown fine roots (SGR), surface soil (approximately 0–20 cm) at the tree base was carefully excavated to expose the primary lateral roots following the procedure described by Guo et al. (2008). For and water-grown fine roots (WGR), whole root systems growing in water were collected. Root branches with intact terminal branch orders were cut, and over 50 g of total fresh biomass of the first three-order roots was obtained from each tree. The function of the first three-order roots is mainly resource absorption (McCormack et al., 2015), and the "fine roots" in this study refer to these absorptive fine roots of the first three orders. Subsamples of the fine roots separated from the root systems were gently washed in low-temperature deionized water to remove soil adhering to the roots.

REFERENCES

Guo, D., Xia, M., Wei, X., Chang, W., Liu, Y., and Wang, Z.: Anatomical traits associated with absorption and mycorrhizal colonization are linked to root branch order in twenty-three Chinese temperate tree species, New Phytol., 180, 673-683, https://doi.org/10.1111/j.1469-8137.2008.02573.x, 2008.

McCormack, M. L., Dickie, I. A., Eissenstat, D. M., Fahey, T. J., Fernandez, C. W., Guo, D., Helmisaari, H. S., Hobbie, E. A., Iversen, C. M., Jackson, R. B., Leppalammi-Kujansuu, J., Norby, R. J., Phillips, R. P., Pregitzer, K. S., Pritchard, S. G., Rewald, B., and Zadworny, M.: Redefining fine roots improves understanding of below-ground contributions to terrestrial biosphere processes, New Phytol., 207, 505-518, https://doi.org/10.1111/nph.13363, 2015.

Text S2 Sequential extraction procedure and GC-MS quantification

Solvent extraction for the dichloromethane and methanol extractable fraction (F_{DcMe}) was performed with 100.0 mg of homogenized root samples (R1), which was extracted with 15 mL dichloromethane (DCM), methanol (MeOH): DCM (1:1, v/v), and MeOH consecutively in 50 mL fluorinated ethylene propylene (FEP) tubes via ultrasonication for 15 min on an ultrasonic instrument (ANPEL 2400TH; frequency of 40 kHz) at 20°C. After centrifugation (3000 *g* for 5 min), the combined solvent extracts were concentrated via rotary evaporation and filtered through a 0.45 μm polyether sulfone filter. The filtrates were dried under N_2 gas in 2 mL glass vials. The remaining samples (non-extractable residues, R2) were air-dried, weighed, and stored at –20°C.

For the base-hydrolyzable fraction (F_{KOHhy}), subsamples of the solvent-extracted residues (R2) were hydrolyzed with 15 mL of freshly prepared 1 mol·L^{-1} methanolic KOH in hydrothermal reactors with 20 mL polytetrafluoroethylene (PTFE) cups at 100°C for 3 h. After cooling to 20°C, the contents were centrifuged, and the supernatants were allowed to evaporate, then they were acidified to pH < 1. The hydrolyzable products were liquid−liquid extracted with 30 mL ethyl acetate three times. The extracts were then concentrated via rotary evaporation and dried under N_2 gas in 2 mL glass vials. The remaining samples (R3) were air-dried, weighed, and stored at −20°C.

For the CuO-oxidizable fraction (F_{CuOox}), subsamples after the base hydrolysis (R3) were oxidized with 1 g CuO, 100 mg $Fe(NH_4)_2(SO_4)_2 \cdot 6H_2O$, and 15 mL of 1 mol·$L^{-1}$ NaOH (pre-sparged with N_2 for 5 min) in PTFE-lined reactors at 170°C for 2.5 h. After cooling to room temperature (20°C), the reaction products were centrifuged; the supernatants were then allowed to evaporate, acidified to pH < 1, and kept in the dark for at least 1 h. The lignin phenols were liquid−liquid extracted with 30 mL ethyl acetate three times. The extracts were then concentrated and dried under N_2 gas in 2 mL glass vials. The remaining samples (R4) were washed with 0.01 mol·L^{-1} HCl to remove any excess CuO and then rinsed with deionized water to remove excess HCl, followed by freeze-drying, weighing, and storing at −20°C.

Aliquots of F_{DcMe} and F_{CuOox} were trimethylsilyl derivatized with *N*,*O*-bis(trimethylsilyl)trifluoroacetamide (BSTFA) at 70°C for 1 h. An aliquot of F_{KOHhy} was first methylated with *N*,*N*-dimethylformamide dimethyl acetal (DMF-DMA) at 60°C for 0.5 h and then trimethylsilyl derivatized. After derivatization, all compounds were analyzed using an Agilent 7890B gas chromatograph equipped with a 5977B mass spectrometer using an HP-5MS column (30 m × 0.25 mm i.d., film thickness, 0.25 μm). The injection volume was 1 μL, and the injection temperature was 300°C. The oven temperature was programmed from 60 to 300°C at a rate of 6°C·min^{-1} and held at 300°C for 20 min. The compounds of F_{DcMe} and F_{KOHhy} were detected in scan mode, with the mass scan range from 50 to 550 Da. F_{CuOox} compounds were detected in selected ion mode based on the method of Kaiser and Benner (2012). For F_{DcMe}, a mixed standard of tetracosane, 1-docosanol, methyl tricosanoate, and ergosterol was used. For aliphatics in F_{KOHhy}, a mixed standard of methyl tricosanoate and methyl oleate was used. For phenolics in F_{KOHhy} and F_{CuOox}, a mixed standard containing a total of 11 lignin phenols (including *p*-hydroxybenzoic acid (PAD), *p*-hydroxyacetophenone (PON), *p*-hydroxybenzaldehyde (PAL), vanillic acid (VAD), acetovanillone (VON), vanillin (VAL), syringic acid (SAD), acetosyringone (SON), syringaldehyde (SAL), *p*-coumaric acid (CAD), and ferulic acid (FAD)) was used.

Also, the total carbon content of root samples (R1) and residues after dichloromethane and methanol extraction (R2), base hydrolysis (R3), and CuO oxidation (R4; Figure 1) were determined using a Vario MACRO cube elemental

analyzer (Elementar, Hanau, Germany). Root ash content was determined as the remaining proportion of root mass after burning at 550°C in a muffle furnace for 4 h.

REFERENCES

Kaiser, K. and Benner, R.: Characterization of lignin by gas chromatography and mass spectrometry using a simplified CuO oxidation method, Anal. Chem., 84, 459-464, https://doi.org/10.1021/ac202004r, 2012.

Table S1 Biomass fractionation and fractional carbon contents based on sequential extraction, and ash content of in soil-grown roots (SGR) and water-grown roots (WGR). Different letters indicate the statistically significant differences ($P < 0.05$) among the four fractions. Asterisks indicate the statistically significant differences ($P < 0.05$) of a certain fraction between SGR and WGR. F_{DcMe}: dichloromethane and methanol extractable fractions; F_{KOHhy}: base-hydrolyzable fractions; F_{CuOox}: CuO-oxidizable fractions.

	SGR					**WGR**				
	F_{DcMe}	F_{KOHhy}	F_{CuOox}	Residue		F_{DcMe}		F_{KOHhy}	F_{CuOox}	Residue
Biomass (%)	8 ± 0 d	34 ± 0 a	33 ± 1 b	25 ± 1 c		13 ± 0 c	*	33 ± 1 a	31 ± 4 a	23 ± 4 b
Carbon (%)	4 ± 1 b	15 ± 0 a	16 ± 0 a	4 ± 0 b		8 ± 0 b	*	16 ± 0 a	15 ± 1 a	5 ± 1 c
Ash (%)	16 ± 2 *					8.6% ± 1.3%				

Table S2 Molecular-level compositions of dichloromethane and methanol extractable fractions (F_{DcMe}) and base-hydrolyzable fractions (F_{KOHhy}) of soil-grown (SGR) and water-grown fine roots (WGR). x-/ω-OH acids: x- or ω-hydroxyalkanoic acids; FAs: saturated normal fatty acids; DAs: saturated normal fatty diacids; UAs: unsaturated normal fatty acid.

			SGR	WGR
FDcMe	phenolics		1.46 ± 0.04	2.25 ± 0.27
		Vanillin	0.15 ± 0	0.33 ± 0.03
		3-Hydroxybenzoic acid	0.24 ± 0.01	0.19 ± 0.04
		4-Hydroxybenzoic acid	0.23 ± 0.03	0.26 ± 0.03
		Protocatechoic acid	0.84 ± 0.06	1.02 ± 0.14
		Ferulic acid	0	0.46 ± 0.06
	glycerolics		3.7 ± 0.17	2.41 ± 0.21
		Glycerol	3.31 ± 0.05	1.75 ± 0.11
		1-Monopalmitin	0.39 ± 0.13	0.66 ± 0.10
	prenolics		5.84 ± 0.63	14.3 ± 1.07
		Dihydroabietic acid	0.13 ± 0.03	0.15 ± 0.03
		β-Guaiene-like	0	0.22 ± 0.04
		β-Guaiene	0.13 ± 0	0.23 ± 0.02
		α-Panasinsen	0.15 ± 0.03	0.31 ± 0.03
		Globulol-like	0.20 ± 0.04	0.29 ± 0.06
		Globulol	1.72 ± 0.22	5.42 ± 0.33
		Terpene-like 1	0.23 ± 0.02	0.27 ± 0.01
		Terpene-like 2	0.21 ± 0.03	0.86 ± 0.07
		Terpene-like 3	0.39 ± 0.07	0
		Terpene-like 4	0.38 ± 0.05	0.47 ± 0.04
		Terpene-like 5	0.59 ± 0.05	1.77 ± 0.17
		Terpene-like 6	0.28 ± 0.04	0.49 ± 0.03
		Andrographolide	0.20 ± 0.02	0.62 ± 0.06
		Terpene-like 7	0.44 ± 0.07	1.17 ± 0.12
		Terpene-like 8	0.45 ± 0.05	1.38 ± 0.11
		Terpene-like 9	0.35 ± 0.09	0.63 ± 0.08
	carbohydrates		9.13 ± 1.09	7.06 ± 0.78
		meso-Erythritol	0.57 ± 0.32	0.50 ± 0.04
		Ribofuranose	0.15 ± 0.01	0.31 ± 0.04
		α-Arabinopyranose	0.13 ± 0	0.17 ± 0.03
		Arabinopyranose	0.15 ± 0.02	0.18 ± 0.03
		Fucopyranose	0.39 ± 0.05	0.29 ± 0.04
		Xylitol	1.36 ± 0.52	1.52 ± 0.13
		Fructofuranose	0.97 ± 0.27	0.33 ± 0.08
		Sorbitol	1.64 ± 0.35	2.00 ± 0.16
		Glucose	1.20 ± 0.09	0.93 ± 0.04
		Myo-Inositol	1.45 ± 0.04	0.37 ± 0.10
		Sucrose	0.51 ± 0.45	0.05 ± 0.08
		Lactose	0.60 ± 0.13	0.41 ± 0.10
	fatty acyls		17.03 ± 1.96	11.82 ± 1.80

		Hexanoic acid	0.92 ± 0.34	0.78 ± 0.09
		Glycolic acid	0.99 ± 0.02	0.57 ± 0.16
		Levulinic acid	0.62 ± 0.07	0.70 ± 0.13
		Hydracrylic acid	0.21 ± 0.19	0.22 ± 0.04
		3-Hydroxybutyric acid	0.61 ± 0.13	0.50 ± 0.05
		Butanedioic acid	0.79 ± 0.13	0.67 ± 0.09
		2,3-Dihydroxy-2-methylpropanoic acid	0.31 ± 0.04	0.43 ± 0.08
		Glyceric acid	0.22 ± 0.08	0.11 ± 0.10
		2-Butenedioic acid	0.28 ± 0.19	0
		Nonanoic acid	0.07 ± 0.12	0.26 ± 0.06
		6-Hydroxyhexanoic acid	0.03 ± 0.05	0
		Doconexent	0.09 ± 0.10	0.22 ± 0.07
		Malic acid	2.25 ± 0.52	0.36 ± 0.20
		Azelaic acid	0.43 ± 0.16	0.54 ± 0.11
		Citric acid	1.20 ± 0.14	0.60 ± 0.16
		Myristic acid	0.33 ± 0.14	0
		Palmitelaidic acid	1.97 ± 0.42	1.21 ± 0.10
		Palmitic Acid	3.37 ± 0.54	2.97 ± 0.24
		Hexadecane-1,2-diol	0.59 ± 0.19	0.46 ± 0.05
		11-Octadecenoic acid	0.74 ± 0.18	0.47 ± 0.07
		Stearic acid	1.02 ± 0.04	0.75 ± 0.20
	steroids		53.83 ± 4.41	125.68 ± 8.80
		11-Ketoetiocholanolone	1.23 ± 0.14	1.13 ± 0.08
		Steroid-like 1	0	1.08 ± 0.06
		Androst-5-ene	0	1.61 ± 0.13
		Steroid-like 2	1.16 ± 0.09	2.55 ± 0.2
		Glycocholate-like 1	1.23 ± 0.09	1.61 ± 0.1
		Acetic acid	1.54 ± 0.15	2.06 ± 0.21
		Steroid-like 3	1.10 ± 0.06	1.80 ± 0.11
		Steroid-like 4	1.32 ± 0.08	2.24 ± 0.21
		Glycocholate-like 2	1.07 ± 0.05	1.72 ± 0.16
		Glycocholate-like 3	2.42 ± 0.43	1.87 ± 0.20
		Steroid-like 5	1.26 ± 0.09	2.85 ± 0.23
		Steroid-like 6	1.10 ± 0.09	2.51 ± 0.17
		Glycocholate-like 4	0	1.21 ± 0.15
		Glycocholate-like 5	1.10 ± 0.10	1.50 ± 0.09
		Campesterol	3.87 ± 0.26	2.56 ± 0.12
		Stigmasterol	3.01 ± 0.11	2.94 ± 0.24
		β-Sitosterol	6.03 ± 0.10	5.06 ± 0.30
		Cholestane-like 1	2.09 ± 0.29	5.79 ± 0.82
		Cholestane-like 2	3.63 ± 1.21	16.35 ± 1.63
		Androstadien-like	17.41 ± 2.28	45.08 ± 2.66
		β-Eudesmol	1.52 ± 0.06	7.91 ± 0.84
		25-Hydroxycholesterol	1.77 ± 0.08	14.25 ± 2.31
FKOHhy	**Aliphatics**		**11.88 ± 1.01**	**9.67 ± 0.27**

	x-OH acids	**0.36 ± 0.04**	**0.28 ± 0.01**
	9, 10-OH 18 FA	0.17 ± 0.03	0.13 ± 0
	2-OH C10 DA	0.18 ± 0	0.15 ± 0
	ω-OH acids	0.64 ± 0.03	0.58 ± 0.01
	ω-OH C16 FA	0.41 ± 0.03	0.38 ± 0.01
	ω-OH C22 FA	0.23 ± 0.01	0.21 ± 0.02
	n-alkanols	1.3 ± 0.18	1.04 ± 0.03
	C22 alkanol	0.62 ± 0.07	0.50 ± 0.01
	C24 alkanol	0.49 ± 0.09	0.38 ± 0.01
	C26 alkanol	0.19 ± 0.02	0.16 ± 0.01
	FAs	**2.02 ± 0.03**	**1.56 ± 0.01**
	C16 FA	1.07 ± 0.07	0.77 ± 0.02
	C18 FA	0.39 ± 0.01	0.32 ± 0.01
	C24 FA	0.18 ± 0.01	0.14 ± 0.01
	C26 FA	0.38 ± 0.02	0.32 ± 0.01
	DAs	**2.01 ± 0.06**	**1.83 ± 0.08**
	C10 DA	0.21 ± 0.01	0.15 ± 0.01
	C11 DA	0.21 ± 0.01	0.15 ± 0.01
	C16 DA	1.18 ± 0.03	1.08 ± 0.08
	C18 DA	0.42 ± 0.03	0.46 ± 0.01
	UAs	**5.56 ± 0.74**	**4.36 ± 0.15**
	9-C16:1 FA	1.47 ± 0.10	1.22 ± 0.07
	9-C18:1 FA	0.45 ± 0.01	0.31 ± 0.01
	11-C18:1 FA	0.49 ± 0.02	0.30 ± 0.01
	9, 12-C18:2 FA	1.47 ± 0.37	1.00 ± 0.05
	9-C20:1 FA	0.45 ± 0.07	0.35 ± 0.01
	10,13-C20:2 FA	0.45 ± 0.13	0.34 ± 0.02
	13-C22:1 FA	0.44 ± 0.06	0.48 ± 0.03
	15-C24:1 FA	0.35 ± 0.02	0.35 ± 0.02
Phenolics		**13.08 ± 0.28**	**25.27 ± 1.84**
	Benzoic acid	0.49 ± 0	0.34 ± 0.01
	p-Hydroxybenzaldehyde	0.54 ± 0.03	0.44 ± 0.01
	p-Hydroxybenzoic acid	0.59 ± 0	0.55 ± 0.03
	Acetovanillone	0.45 ± 0.02	0.55 ± 0.04
	Vanillic acid	2.65 ± 0.18	4.98 ± 0.40
	Vanillin	1.02 ± 0.09	2.73 ± 0.18
	iso-Vanillin	0.49 ± 0.02	1.17 ± 0.09
	Syringic acid	1.05 ± 0.05	0.63 ± 0.04
	Syringaldehyde	0.38 ± 0.02	0.37 ± 0.01
	p-Coumaric acid	0.53 ± 0.24	0.41 ± 0.02
	Ferulic acid	3.31 ± 0.18	11.13 ± 0.91
	iso-Ferulic acid	0.55 ± 0.02	0.95 ± 0.15
	Bisphenol1	0.37 ± 0.04	0.43 ± 0.06
	Bisphenol2	0.32 ± 0.01	0.33 ± 0.01
	Bisphenol3	0.37 ± 0.02	0.25 ± 0

Table S3 Chemical properties (means ± standard errors) of CuO-oxidizable fractions (F_{CuOox}) of different fine-root samples. The *P*-value indicates the significance level of a two-way *t*-test between soil-grown roots (SGR) and water-grown roots (WGR).

	Abbreviations	**Units**	**SGR**	**WGR**	***P*-values**
Total 11 phenol yield	Λ11	mg g C^{-1}	24.21 ± 5.25	30.93 ± 2.95	0.125
Total lignin phenol yield	Λ8	mg g C^{-1}	23.32 ± 4.86	29.07 ± 2.56	0.144
p-hydroxy phenol yield	*P*	mg g C^{-1}	0.89 ± 0.38	1.86 ± 0.45	0.047
Vanillyl phenol yield	*V*	mg g C^{-1}	15.63 ± 3.23	21.23 ± 2.33	0.072
Syringyl phenol yield	*S*	mg g C^{-1}	6.81 ± 1.61	6.97 ± 0.87	0.890
Cinnamyl phenol yield	*C*	mg g C^{-1}	0.87 ± 0.54	0.87 ± 0.58	0.999
Vanillyl : lignin phenol ratio	*V*:Λ8	-	0.67 ± 0.01	0.73 ± 0.02	0.009
Syringyl: lignin phenol ratio	*S*:Λ8	-	0.29 ± 0.01	0.24 ± 0.01	0.009
Cinnamyl: lignin phenol ratio	*C*:Λ8	-	0.04 ± 0.02	0.03 ± 0.02	0.729
Syringyl : vanillyl phenol ratio	*S*:*V*	-	0.43 ± 0.02	0.33 ± 0.02	0.002
Cinnamyl : vanillyl phenol ratio	*C*:*V*	-	0.06 ± 0.04	0.04 ± 0.03	0.641
Acid : aldehyde for vanillyl phenols	$(Ad:Al)_V$	-	0.38 ± 0.05	0.46 ± 0.02	0.056
Acid : aldehyde for syringyl phenols	$(Ad:Al)_S$	-	0.40 ± 0.03	0.53 ± 0.05	0.020

Table S4 The number of assigned formulae and the sum of assigned signal of three replicates, and the number of formulae and percentage of signal of their common formulae. F_{DcMe}: dichloromethane and methanol extractable fractions; F_{KOHhy}: base-hydrolyzable fractions; F_{CuOox}: CuO-oxidizable fractions.

			SGR			WGR		
			F_{DcMe}	F_{KOHhy}	F_{CuOox}	F_{DcMe}	F_{KOHhy}	F_{CuOox}
Replicate-1	Number of assigned formulae		3913	2674	4285	3078	2383	2347
	Sum of assigned signal		1.72E+11	1.42E+11	1.76E+11	1.10E+11	6.28E+10	5.24E+10
Replicate-2	Number of assigned formulae		3445	3029	4546	3381	3021	2254
	Sum of assigned signal		1.90E+11	1.60E+11	1.72E+11	1.10E+11	8.37E+10	5.71E+10
Replicate-3	Number of assigned formulae		3252	2608	4214	3457	2662	2201
	Sum of assigned signal		1.37E+11	1.53E+11	1.48E+11	1.31E+11	7.48E+10	5.04E+10
Common formulae	Number of formulae		2500	2070	3380	2594	1962	1746
	Percentage of signal	replicate-1	78%	92%	87%	90%	95%	93%
		replicate-2	88%	74%	94%	91%	90%	94%
		replicate-3	93%	86%	94%	86%	93%	94%

Table S5 Molecular characterization of sequentially extractable fractions in soil-grown roots (SGR) and water-grown roots (WGR), as determined using Fourier transform ion cyclotron resonance mass spectrometry (FT-ICR MS). "wa" indicates intensity weighted average value. Different letters indicate the statistically significant differences ($P < 0.05$) among the three fractions. Asterisks indicate the statistically significant differences ($P < 0.05$) of a certain fraction between SGR and WGR. F_{DcMe}: dichloromethane and methanol extractable fractions; F_{KOHhy}: base-hydrolyzable fractions; F_{CuOox}: CuO-oxidizable fractions. CHO: formulae containing only carbon, hydrogen, and oxygen; CHON: formulae containing only carbon, hydrogen, oxygen, and nitrogen; CHOS: formulae containing only carbon, hydrogen, oxygen, and sulfur; CHONS: formulae containing only carbon, hydrogen, oxygen, nitrogen, and sulfur.

	SGR									**WGR**								
	F_{DcMe}			F_{KOHhy}			F_{CuOox}			F_{DcMe}			F_{KOHhy}			F_{CuOox}		
Number of assigned formulae	3537 ± 340	b		2770 ± 226	c		4348 ± 175	a	*	3305±201	a		2689 ± 320	b		2267 ± 74	b	
m/z_{wa}	359 ± 10	a		359 ± 13	a		366 ± 1	a		362 ± 2	a		365 ± 4	a		367 ± 1	a	
H/C_{wa}	1.68 ± 0.00	a	*	1.59 ± 0.02	b	*	1.56 ± 0.02	c	*	1.38 ± 0.02	a		0.93 ± 0.01	b		0.87 ± 0.00	c	
O/C_{wa}	0.33 ± 0.01	a		0.34 ± 0.01	a		0.35 ± 0.01	a		0.38 ± 0.01	c	*	0.52 ± 0.01	b	*	0.54 ± 0.01	a	*
DBE_{wa}	4.07 ± 0.11	c		4.79 ± 0.08	b		5.14 ± 0.20	a		6.61 ± 0.24	c	*	10.34 ± 0.07	b	*	10.81 ± 0.09	a	*
$AI_{mod\ wa}$	0.09 ± 0.00	c		0.12 ± 0.01	b		0.14 ± 0.01	a		0.23 ± 0.01	c	*	0.46 ± 0.00	b	*	0.49 ± 0.00	a	*
$NOSC_{wa}$	-0.98 ± 0.03	c		-0.89 ± 0.04	b		-0.8 ± 0.04	a		-0.58 ± 0.04	c	*	0.12 ± 0.01	b	*	0.23 ± 0.03	a	*
Number of CHO (%)	54 ± 2	b		58 ± 1	a		50 ± 0	c		58 ± 2	b		64 ± 5	a		68 ± 1	a	*
Abundance of CHO (%)	84 ± 0	a		87 ± 2	a		86 ± 1	a		91 ± 0	a	*	89 ± 2	a		90 ± 0	a	*
Number of CHON (%)	34 ± 1	b		36 ± 1	b		44 ± 1	a	*	40 ± 1	a	*	34 ± 5	ab		30 ± 1	b	
Abundance of CHON (%)	8 ± 1	b		12 ± 3	a		12 ± 1	a	*	9 ± 0	a		11 ± 2	a		9 ± 0	a	
Number of CHOS (%)	12 ± 1	a	*	6 ± 1	b	*	6 ± 1	b	*	3 ± 0	a		1 ± 0	b		2 ± 1	ab	
Abundance of CHOS (%)	6 ± 1	a	*	2 ± 0	b	*	2 ± 0	b	*	<1	a		<1	a		<1	a	
Number of CHONS (%)	1 ± 0	a	*	<1	b		<1	b		<1	a		<1	a		<1	a	
Abundance of CHONS (%)	1 ± 0	a	*	<1	b		<1	b		<1	a		<1	a		<1	a	

Table S6 Morphology and chemical properties (means ± standard errors) of different fine-root samples. The *P*-value indicates the significance level of a two-way *t*-test between soil-grown roots (SGR) and water-grown roots (WGR).

	Units	**SGR**	**WGR**	***P*-values**
Average diameter	mm	1.18 ± 0.02	1.70 ± 0.10	0.003
Specific root length	m g^{-1}	6.00 ± 0.22	2.63 ±0.20	< 0.001
Root tissue density	g cm^{-3}	0.15 ±0.01	0.17 ± 0.00	0.101
Carbon content	mg g $root^{-1}$	390 ±4	440 ± 2	< 0.001
Nitrogen content	mg g $root^{-1}$	18.2 ± 0.10	16.3 ± 0.03	0.013
Carbon nitrogen ratio	-	27.0 ± 0.35	21.4 ± 0.80	< 0.001

Table S7 Two-way ANOVA for the effects of redox condition, root class and their interaction on root carbon remaining during root decomposition.

	Carbon remaining	
	F	*P*
Redox condition	241.05	< 0.001
Root type	162.94	< 0.001
Redox condition × Root type	0.14	0.714

Figure S1 One of the mature trees of *Dysoxylum binectariferum* Hook. f growing by a slow flowing stream and its soil-grown (SGR) and water-grown fine roots (WGR). WGR had observably different morphology, such as larger diameter and less branches. These photographic materials were taken by Mengke Wang.

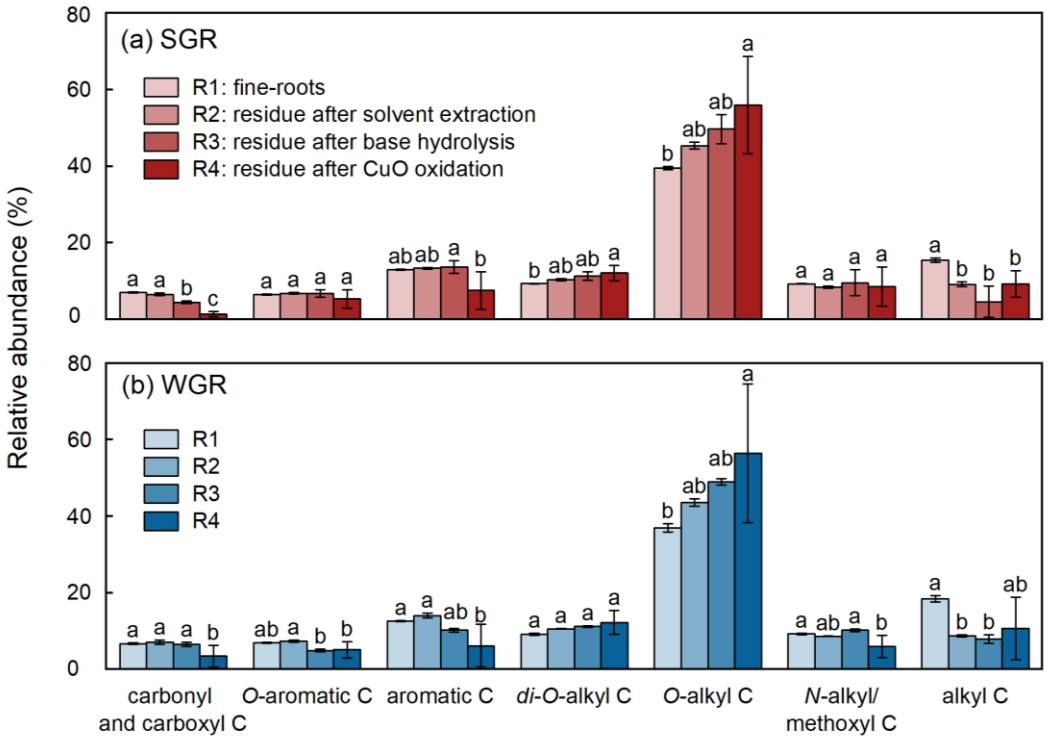

Figure S2 Solid-state ^{13}C cross-polarization magic angle spinning nuclear magnetic resonance integration results for SGR (a) and WGR (b) samples before and during sequential extraction with a variety of extraction procedures. Bars represent mean ± standard error (n = 3). Different letters at the top of each bar indicate significant differences ($P < 0.05$) in percentages of carbon regions among different solid phases after sequential extraction. Four colors from light to dark indicate original fine-root samples (R1) and residues after solvent extraction (R2), base hydrolysis (R3), and CuO oxidation (R4). The carbonyl and carboxyl C, *O*-aromatic C, aromatic C, *di*-*O*-alkyl C, *O*-alkyl C, *N*-alkyl/methoxy C, and alkyl C are restricted within chemical shifts (ppm) of 165–210, 145–165, 110–145, 95–110, 60–95, 45–60, and 0–45, respectively.

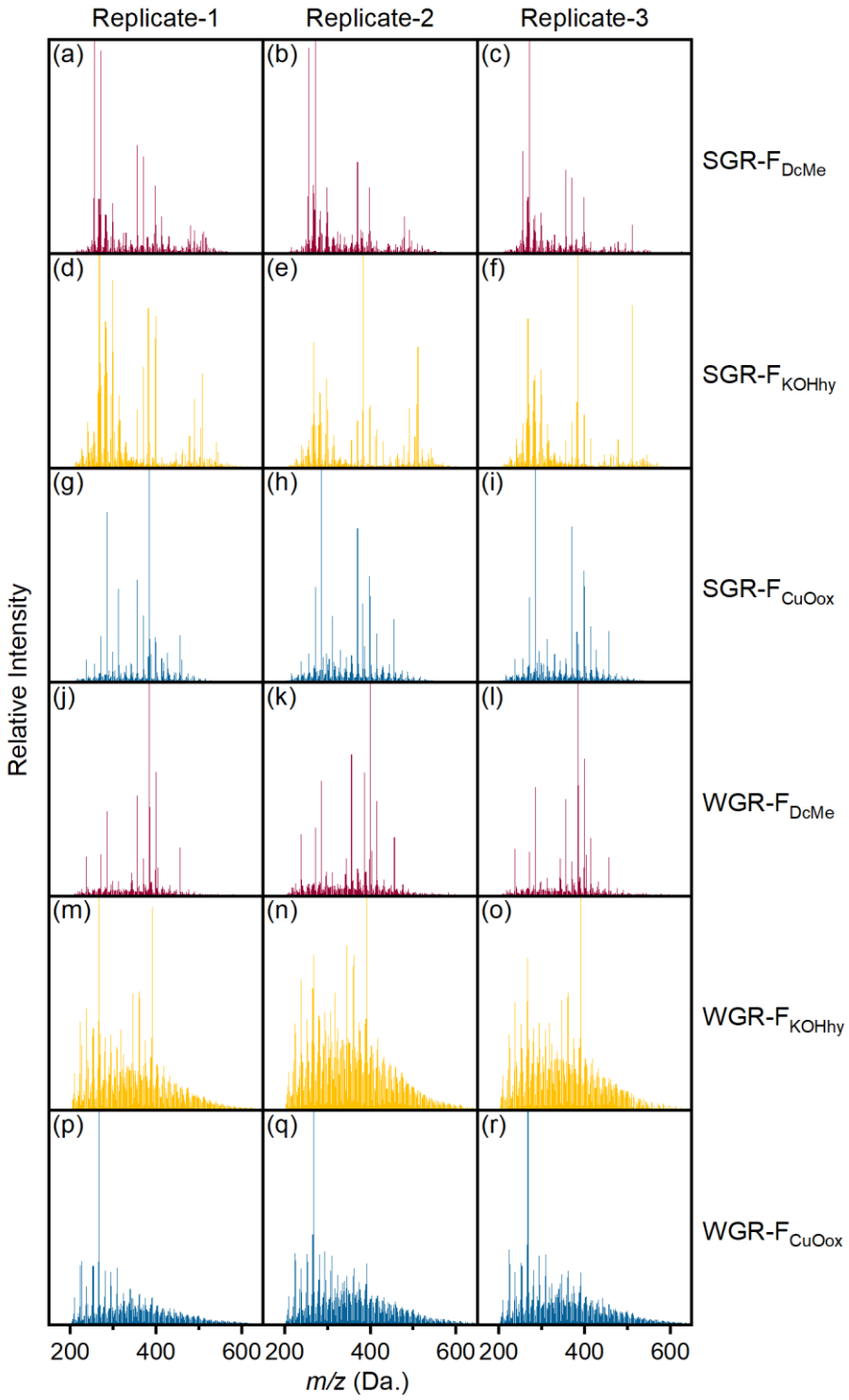

Figure S3 Fourier transform ion cyclotron resonance mass spectra (FT-ICR MS) of the different extractable fractions of organic matter in three replicates of f soil-grown roots (SGR, a-i) and water-grown roots (WGR, j-r). F_{DcMe}: dichloromethane and methanol extractable fractions; F_{KOHhy}: base-hydrolyzable fractions; F_{CuOox}: CuO-oxidizable fractions.

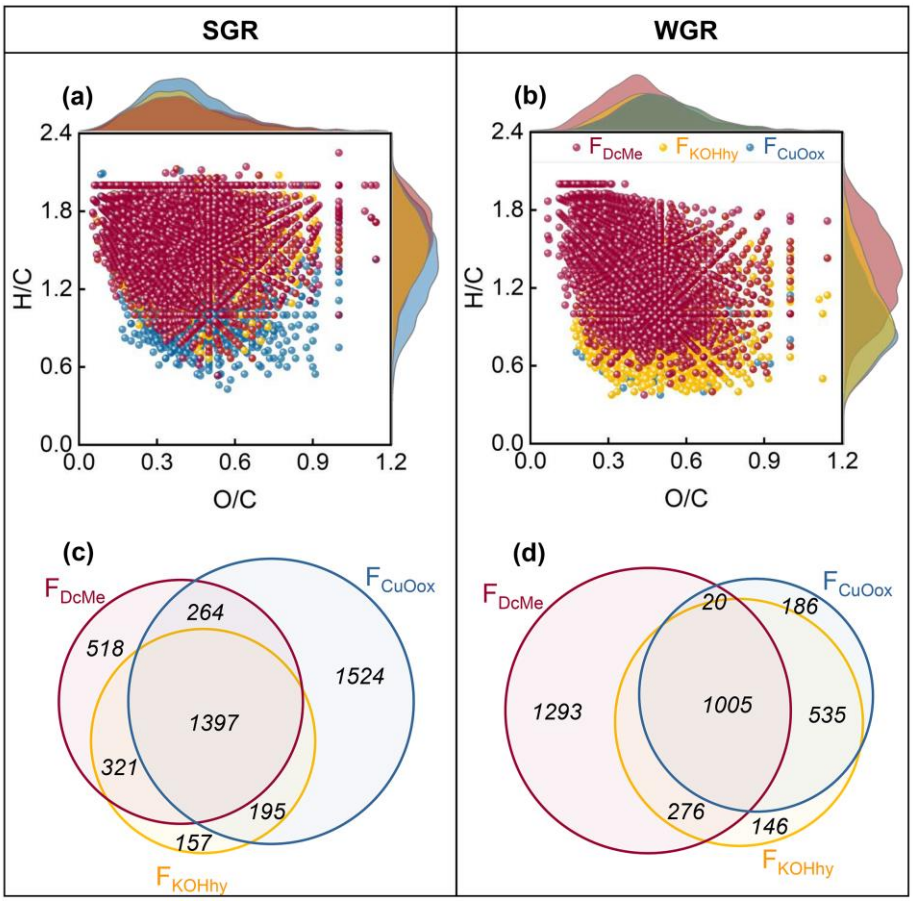

Figure S4 van Krevelen and Venn diagrams of Fourier transform ion cyclotron resonance mass spectrometry (FT-ICR MS)-detected formulae from sequentially extracted fractions of soil-grown roots (SGR; a, c) and water-grown roots (WGR; b, d). F_{DcMe}: dichloromethane and methanol extractable fractions; F_{KOHhy}: base-hydrolyzable fractions; F_{CuOox}: CuO-oxidizable fractions. Note that the formulae in van Krevelen diagrams (**a, b**) are the common formulae existing in all three replicates, and the percentage of number and signal of these common formulae in the total number and total signal were on average 76% and 90%, respectively (Table S3).